Arch. Mech., 43, 1, pp. 3–27, Warszawa 1991

Constitutive scheme of discrete memory form for granular materials (*)

P. PEGON (ISPRA), P. GUELIN, D. FAVIER, B. WACK (GRENOBLE), and W. K. NOWACKI (WARSZAWA)

THE PURE HYSTERESIS model, which is at the origin of a class of well-founded thermomechanical schemes of discrete memory form is briefly recalled and then expanded to include the isotropic-deviatoric coupling effects. Thus the model takes into account the essential features of the elastic-plastic and pressure-dependent behaviour of cohesive or cohesionless continua subjected to arbitrary cyclic loadings.

Przedstawiono pokrótce model idealnej histerezy, który jest podstawą całej klasy dobrze postawionych termomechanicznych schematów o postaci pamięci dyskretnej. Przedstawiono następnie jego rozszerzenie, uwzględniając efekty sprzężenia izotropowo-dewiatorowego. Model ten uwzględnia zachowanie się sprężysto-plastyczne oraz zależne od ciśnienia materiałów sypkich poddanych dowolnym obciążeniom cyklicznym.

Вкратце представлена модель идеального гистерезиса, которая является основой целого класса хорошо поставленных термомеханических схем с видом дускретной памяти. Затем представлено ее расширение, учитывая эффекты изотропно-девиаторного сопряжения. Эта модель учитывает упруго-пластическое поведение и зависящие от давления поведение сыпучих материалов, подвергнутых произвольным циклическим нагрузкам.

Notations

$(0, \mathbf{e}_\alpha)$	orthonormal fixed reference frame ($\alpha = 1, 2, 3$),
t	absolute time,
$\frac{\partial}{\partial t}$ or $\dot{}$	partial derivation with respect to t,
M	material point,
$x^i (i = 1, 2, 3)$	curvi-linear material coordinates dragged with the body,
$\mathbf{p}(M, t)$	current position of $M (\mathbf{p} = z^\alpha(x^i, t)\mathbf{e}_\alpha)$,
$\mathbf{g}_i(M, t)$	current reference frame associated with the $x^i \left(\mathbf{g}_i = \frac{\partial z^\alpha}{\partial x^i}\mathbf{e}_\alpha\right)$,
$g_{ij}(M, t)$	current covariant components of the metric tensor g,
$\sqrt{g(M, t)}$	current density of volume per unit of material volume with $g = \det \lvert g_{ij} \rvert$,
$D(M, t)$	current strain rate tensor $\left(D_{ij} = \frac{1}{2}\frac{\partial g_{ij}}{\partial t}\right)$,
I_D	trace of $D \left(= D^i{}_i = \frac{1}{\sqrt{g}}\frac{\partial \sqrt{g}}{\partial t}\right)$,
t_R	inversion time associated with the origin of a branch of cycle,
${}^t_R g(M, t)$	current Cauchy strain dragged along from t_R to t,
$\Delta {}^t_R \varepsilon(M, t)$	current (Almansi) strain $\left(= \frac{1}{2}(g - {}^t_R g)\right)$,
$\sigma(M, t)$	current Cauchy stress (relative of weight 1),
${}^t_R \sigma(M, t)$	current Cauchy stress dragged along from t_R to t,

(*)Paper presented at VIIth French-Polish Symposium "Recent trends in mechanics of elasto-plastic materials", Radziejowice, 2–7 VII, 1990.

$\Delta_R^t\sigma(M,t)$ current variation of stress from t_R to t ($\Delta_R^t\sigma = \sigma - {}_R^t\sigma$),
$S, {}_R^tS, \Delta_R^tS$ current absolute tensors associated with $\sigma, {}_R^t\sigma, \Delta_R^t\sigma$ ($\sigma = S\sqrt{g}$),
$\overline{S}$ deviatoric part of the current Cauchy stress S,
$I_S, \overline{II}_{\bar{S}}, \overline{III}_{\bar{S}}$ current invariants $S^i{}_i, \frac{1}{2}\overline{S}^i{}_j\overline{S}^j{}_i, \frac{1}{3}\overline{S}^i{}_j\overline{S}^j{}_k\overline{S}^k{}_i$,
p current pressure $\left(p = \frac{I_s}{3}\right)$,
Q_s, φ_s current values of $2\overline{II}_{\bar{s}}$ and of the phase such as $\cos 3\varphi_s = \frac{3\sqrt{6}\overline{III}_{\bar{s}}}{Q_s^3}$,
Q_R, φ_R current values of Q and φ for the tensor ${}_R^tS$,
Q_Δ, φ_Δ current values of Q and φ for the tensor Δ_R^tS,
$M1$ $\Delta\sigma D$ in the one-dimensional case,
$\overline{M}, \overline{N}$ current mixed invariants $\overline{\Delta_R^tS^i{}_j}\overline{D^j{}_i}$ and $\overline{\Delta_R^tS^i{}_j}\,\overline{\Delta_R^tS^j{}_k}\,\overline{D^k{}_i}$,
$\varrho(M,t)$ current specific mass ($\varrho\sqrt{g} = c\,\text{ste}$),
$\mathcal{P}_{\text{int}}, P_{\text{int}}, p_{\text{int}}$ current power of internal forces ($\mathcal{P}_{\text{int}} = P_{\text{int}}\sqrt{g} = \varrho p_{\text{int}}\sqrt{g}$),
$\mathcal{E}, E, e$ current internal energy,
$\mathcal{Q}_{ii}, Q_{ii}, q_{ii}$ current internal intrinsic heat supply,
$\Pi, P_{\text{rev}}, p_{\text{rev}}$ current reversible power,
$\Phi, \overline{\Phi}, \varphi$ current intrinsic dissipation ($\Phi = -\mathcal{P}_{\text{int}} - \Pi$),
λ_0, μ_0 Lamé parameters (absolute scalars),
S_0, Q_0 von Mises parameters (limit shear stress S_0 and radius $Q_0 = \sqrt{2}S_0$ of the von Mises cylinder),
j, k rank j of an arc in the branch of rank k,
$\delta, \mathbf{1}$ Kronecker symbol, unit tensor ($g^{\bullet}{}_{\bullet} = g_{\bullet}{}^{\bullet} = \mathbf{1}$),
def definition,
$\omega(M,t)$ Massing functional ($\omega = 1$ or 2).

1. Introductory remarks

THE MAIN EXPERIMENTAL results concerning the behaviour of sand-like materials may be summarized as follows:

i) the yielding is dependent upon the confining stress,

ii) careful measurements show that a burst of heat flux is associated with yielding [1],

iii) under deviatoric stress states, the volume most often expands after an initial small compaction,

iv) under deviatoric cyclic loading, each inversion of the loading gives rises to a compaction even if the associated confining stress decreases,

v) under hydrostatic compression, the behaviour exibits hysteresis and is "nonlinear",

vi) the yielding is not of von Mises type but rather of "generalized Columb"-type, and may be anisotropic.

The main purpose of this paper is to define a constitutive scheme taking into consideration the first four results (points i to iv). The study is therefore basically devoted to the problem of the isotropic-deviatoric coupling effects: the hysteresis exibited under purely hydrostatic loading is neglected as well as the Coulomb yield effect and the anisotropic effect ([1]).

A simple hint regarding the form of the proposed scheme may be introduced as follows. The scheme is defined firstly through an isotropic part:

$$\dot{I}_s = (3\lambda + 2\mu)I_D + \alpha\overline{M}_p \tag{1.1}$$

([1]) It is worth to notice that the hydrostatic hysteresis may be taken into account on the basis of the proposed method and that the Coulomb effects has been already studied in the case of non-rotational kinematics [2]. Moreover, the extension of the theory to the anisotropic case is from now on outlined.

including a scalar functional $\overline{M}_p$ similar to $\overline{M}$, and secondly with the aid of a deviatoric part:

$$\dot{\overline{S}}^i{}_j = 2\mu\overline{D}^i{}_j + \beta\overline{\Phi}\Delta^t_R\overline{S}^i{}_j \quad \text{in} \quad (0, \mathbf{e}_\alpha)(^2) \tag{1.2}$$

which is of pure hysteresis type and has been defined previously (see for example Subsect. 1.3 of [5] or [2, 3]).

In these differential-difference equations λ and μ are scalar functions of the pressure p; α is a scalar functional deviatoric stress invariant; $\overline{M}_p$ is an extension of the functional invariants $\overline{M}$ to the case of pressure-dependent processes; β is a scalar functional of $(\varphi_\Delta - \varphi_R)$; $\overline{\Phi}$ is the scalar functional:

$$\overline{\Phi} \overset{\text{def}}{=} \Delta^t_R\overline{S}_p{}^{ij}\overline{D}_{ji} + \gamma\dot{\varphi}_\Delta + \Gamma\dot{p} \tag{1.3}$$

linear with respect to the rates $\dot{p}$, $\dot{\varphi}_\Delta$.

In relation (1.3), $\Delta^t_R\overline{S}_p$ is an expansion of the variation $\Delta^t_R S$; it gives the definition of the functional invariant:

$$\overline{M}_p \overset{\text{def}}{=} \Delta^t_R\overline{S}_p{}^{ij}\overline{D}_{ji}$$

which plays a central role in the definition of the whole pattern.

Such a very short hint may be sufficient if the origin and the general features of the three-dimensional scheme of pure hysteresis is already well known on the basis of extensive analysis ([2, 3, 4]) or through various short papers ([5] to [10]). However, when dealing with the question of the isotropic-deviatoric coupling effects, it is worth to ensure that the paper is widely self-contained regarding the tensorial formalism. Consequently, the simplest three-dimensional deviatoric tensorial scheme is recalled (Sect. 2). The main part of the paper is devoted to the extension of the scheme (Sect. 3). In order to obtain the first set of illustrations, integrations are performed using kinematical conditions similar to those of the usual modern experiments (Sect. 4). A second set of illustrations is introduced regarding the properties of the proposed scheme under small, medium and large cyclic loading (Sect. 5).

2. The simplest tensorial deviatoric scheme of pure hysteresis

2.1. Introduction based on a one-dimensional symbolic model

As already underlined ([2] to [8, 13] and [14]), the main feature of the behaviour of pure hysteresis are its stationary properties during periodic cyclic loading. The term stationary is of straightforward meaning in the one-dimensional case briefly recalled below, and it is not essential to give here a more general definition. Therefore, the only readily suggested patterns are those provided by the symbolic models consisting of an infinite number of springs and friction sliders, for example ordered in an infinite parallel succession of spring and slider couples associated in series (Fig. 1) ([3]).

Let $g(e)$ be the function of the deformation e defined on Fig. 2. It is well known that $g''(e)de$ is the rigidity coefficient for the pairs having their limit values between e and

([2]) The simple choice of $(0, \mathbf{e}_\alpha)$ as frame of definition is obviously provisional as stressed below (cf. Sect. 6).

([3]) It is worth to notice that this symbolic model and the associated pure hysteresis notion is not groundless at the physically relevant scale (cf. Appendix).

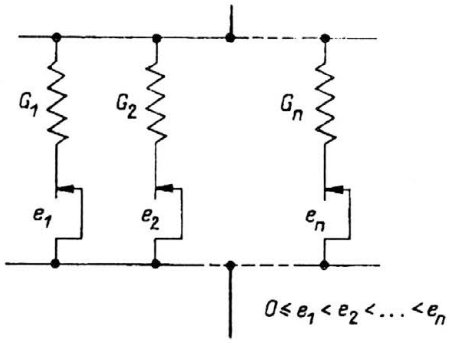

FIG. 1. One-dimensional symbolic model.

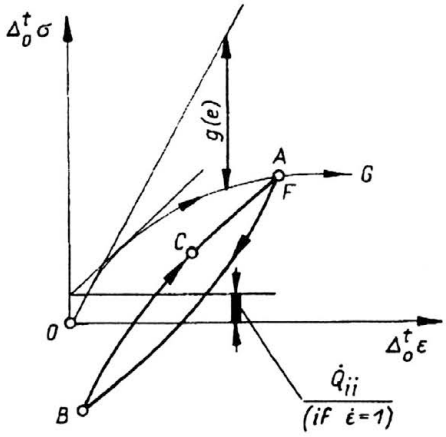

FIG. 2. Behaviour of the symbolic model.

$(e + de)$, and

$$\sigma = \sigma_1 + \sigma_2, \quad \sigma_1 = \int_{\varepsilon}^{\infty} \varepsilon g''(e)\, de, \quad \sigma_2 = \int_{0}^{\varepsilon} e g''(e)\, de$$

along the first loading path. In these relations σ_1 is associated with pairs whose limit value is not reached and σ_2 to pairs whose limit value is reached. Then one has *along the first loading branch*

$$\left| \begin{aligned} &\sigma = G_0\varepsilon - \int_0^{\varepsilon} (\varepsilon - e) g''(e)\, de = G_0\varepsilon - g(\varepsilon) = S(\varepsilon), \\ &G_0 = \int_0^{\infty} g''(e)\, de = g'(\infty), \quad g'' = -\sigma'' \geq 0. \end{aligned} \right. \tag{2.1}$$

It is interesting to add some elementary calculation [9] regarding the power associated with the pairs whose limit value is not reached (this gives the rate of internal energy) and the power associated with the other pairs (this gives the rate of heat flow due to the

friction sliders). Consequently, one starts from

$$-\mathcal{P}_{\text{int}} = \sigma_1 D + \sigma_2 D, \quad \dot{\mathcal{E}} = \sigma_1 D, \quad -\dot{Q}_{ii} = \sigma_2 D$$

and, after integration and substitution of g, one obtains

$$\dot{\mathcal{E}}(\varepsilon) = \varepsilon\dot{\sigma}(\varepsilon), \quad -\dot{Q}_{ii}(\varepsilon) = \sigma(\varepsilon)\dot{\varepsilon} - \varepsilon\dot{\sigma}(\sigma). \tag{2.2}$$

The discrete memory notion is introduced when one considers the path $O-A-B-C-F-G$ (Fig. 2): the $A-B-F$ cycle is forgotten along the $F-G$ path which is identical to what it would have been if the loading had been monotone.

Along the path $A-B$ one has [10]:

$$\Delta_A^t\sigma = \int_{\Delta_A^t\varepsilon/2}^{\infty} \Delta_A^t\varepsilon g''(e)\,de + \int_0^{\Delta_A^t\varepsilon/2} 2eg''(e)\,de$$

$$= 2\left[G_0\frac{\Delta_A^t\varepsilon}{2} - g\left(\frac{\Delta_A^t\varepsilon}{2}\right)\right] = 2S\left(\frac{\Delta_A^t\varepsilon}{2}\right).$$

Then introducing the similarity functional ω, one has for any branch the following expansion of Eqs. (2.1):

$$\Delta_R^t\sigma = \omega S\left(\frac{\Delta_R^t\varepsilon}{\omega}\right), \quad \omega = 1 \text{ or } 2. \tag{2.3}$$

To this straightforward calculation may be added the associated extension of Eqs. (2.2) to the cyclic case [11],

$$\left|\begin{aligned} &\omega\dot{\mathcal{E}}(\Delta_R^t\varepsilon) = ((\omega-1)\sigma + {}_R^t\sigma)\frac{\partial}{\partial t}\Delta_R^t\varepsilon + \Delta_R^t\varepsilon\frac{\partial}{\partial t}\Delta_R^t\sigma, \\ &-\omega\dot{Q}_{ii}(\Delta_R^t\varepsilon) = \Delta_R^t\sigma\frac{\partial}{\partial t}\Delta_R^t\varepsilon - \Delta_R^t\varepsilon\frac{\partial}{\partial t}\Delta_R^t\sigma. \end{aligned}\right. \tag{2.4}$$

Obviously, the previous definitions of $\dot{\mathcal{E}}$ and $\dot{Q}_{ii}$ satisfy the energy balance. In Eqs. (2.3) and (2.4), the process of dragging along the branch is implicitly introduced through

$$\left|\begin{aligned} &\frac{\partial}{\partial t}{}_R^t\varepsilon = 0 \quad (\Delta_R^t\varepsilon = \varepsilon - {}_R^t\varepsilon), \\ &\frac{\partial}{\partial t}{}_R^t\sigma = 0 \quad (\Delta_R^t\sigma = \sigma - {}_R^t\sigma). \end{aligned}\right. \tag{2.5}$$

Now at least two remarks of both theoretical and practical importance must be outlined. The first one states that if the S function is selected following the elastic-perfectly plastic pattern with the aid of the hyperbolic tangent, Eqs. (2.3) and (2.5) yield

$$\frac{\partial}{\partial t}\Delta_R^t\sigma = \frac{\partial\sigma}{\partial t} = G_0\left[1 - \frac{(\Delta_R^t\sigma)^2}{(\omega S_0)^2}\right]\frac{\partial\varepsilon}{\partial t} \tag{2.6}$$

if $S(u)$ is defined by $S_0\text{th}\left(\frac{G_0 u}{S_0}\right)$. Then

$$\frac{\partial\sigma}{\partial t} = G_0 D + \left(\frac{-G_0}{(\omega S_0)^2}\right)\Phi\Delta_R^t\sigma, \quad \Phi = \Delta_R^t\sigma D = M1$$

or

$$\frac{\partial\sigma}{\partial t} = G_0 D + \beta\Phi\Delta_R^t\sigma, \quad \Phi = \Delta_R^t\sigma D = M1. \tag{2.7}$$

The second remark is that the functional Φ, distinguished in the differential-difference equation (2.6), is the intrinsic dissipation ($\Phi \geq 0$) resulting firstly from the analysis of the quasi-reversibility at the right of the vicinity of the inversion point A (Fig. 2):

$$\Pi = {}^{t}_{A}\sigma D\,, \quad t = t_{A+}$$

and, secondly, from the conceptual departure from the classical thermostatics obtained by keeping the same form along the finite branch [11]:

$$\Pi = {}^{t}_{A}\sigma D\,, \quad t \in]t_A, t_B]\,.$$

The two main practical consequences are first, that the inversion criterion is

$$\text{if } \delta W_A = \Phi \delta t < 0 \;\forall t \in]t, t+\delta t] \Rightarrow t = t_I\,, \quad \sigma(t) = \sigma_I \tag{2.8}$$

and secondly that the "help function":

$$W = \frac{2W_A}{\omega^2}\,, \quad dW_A = \Phi\, dt\,, \quad W_A(t_{R+}) = 0 \tag{2.9}$$

allows to define an algorithm $\mathcal{A}$ giving ω, ${}^{t}_{R}\sigma$ and the set of still memorized variables $\{{}^{t}_{M}W\}$ and $\{{}^{t}_{M}\sigma\}$.

Consequently the *pure hysteresis scheme* is given by the combination of five conditions (2.10):

1) *Discrete memory existence* (similar to Eqs. (2.5))

$$\frac{\partial}{\partial t}\,{}^{t}_{R}\varepsilon = \frac{\partial}{\partial t}\,{}^{t}_{R}\sigma = 0\,. \tag{2.10}_1$$

2) *Constitutive differential-difference equations* regarding mechanical and thermomechanical properties and similar to (2.6) and (2.4),

$$\left|\begin{array}{l} \dfrac{\partial \sigma}{\partial t} = f\left(\Delta\,{}^{t}_{R}\varepsilon, \dfrac{\partial \Delta\,{}^{t}_{R}\varepsilon}{\partial t}, \Delta\,{}^{t}_{R}\sigma, \omega\right)\,, \\[2ex] \begin{bmatrix} \Pi \\ -\dot{Q}_{ii} \\ \dot{\mathcal{E}} \end{bmatrix} = \begin{bmatrix} -1 & -1 & 0 \\ 0 & \dfrac{1}{\omega} & -\dfrac{1}{\omega} \\ -1 & -\dfrac{1}{\omega} & \dfrac{1}{\omega} \end{bmatrix} \begin{bmatrix} \mathcal{P}_{\text{int}} \\ \Phi \\ \mathcal{C} \end{bmatrix}\,, \quad \mathcal{C} = \Delta\,{}^{t}_{R}\varepsilon \dfrac{\partial \Delta\,{}^{t}_{R}\sigma}{\partial t}\,, \end{array}\right. \tag{2.10}_2$$

where $\mathcal{C}$ is the basic calorific rate of pure hysteresis.

3) *Inversion criterion* (2.8), which is identical with the second law of thermodynamics.

4) *Algorithm* expressing the minimum increase of the intrinsic dissipation rate $\partial\Phi/\partial t$:

$$\dot{\Phi}(A_+) = \min\{\dot{\Phi} \text{ already memorized at } A\}$$

and practically defined by using W. This algorithm has the following form:

$$\mathcal{A} = \left\{\begin{array}{l} \delta W \overset{?}{<} 0 \Longrightarrow \mathcal{A}_1 \\ \delta W \overset{?}{\geq} 0 \Rightarrow \left|\begin{array}{l} (W(t) - W_n) \overset{?}{\leq} 0 \Longrightarrow \mathcal{A}_m \\ (W(t) - W_n) \overset{?}{>} 0 \Rightarrow \left|\begin{array}{l} W(t) - W_2 \overset{?}{\leq} 0 \Rightarrow \mathcal{A}_c \\ \overset{?}{>} 0 \Rightarrow A_{c0} \end{array}\right. \end{array}\right. \end{array}\right. \tag{2.10}_3$$

with

$$\left|\begin{array}{l} \mathcal{A}_i \xrightarrow{\text{inversion}} \left|\begin{array}{l} \omega = 2,\ k = k+1,\ j = 1, \\ n = n+1,\ {}_R^t\sigma = \sigma_n (= \sigma(t)),\ {}_R^tW = W_n (= W(t)), \end{array}\right. \\ \mathcal{A}_m \xrightarrow{\text{monotony}} \mathbf{1} \text{ (symbolic) along arch } j \text{ of branch } k, \\ \mathcal{A}_c \xrightarrow{\text{crossing}} \omega = 2,\ k = k,\ j = j+1,\ n = n-2,\ {}_R^t\sigma = \sigma_n,\ {}_R^tW = W_n, \\ \mathcal{A}_{c0} \xrightarrow[\text{first loading}]{\text{comeback on}} \omega = 1,\ k = k,\ j = j+1,\ n = 1,\ {}_R^t\sigma = \sigma_1 = 0,\ {}_R^tW = W_1 = \infty, \end{array}\right.$$

and

$$\left|\begin{array}{l} \{{}_M^tW\}_n = \{W_1, \ldots, W_n\} = \{\infty, W(t_0), \ldots\}_n, \\ \qquad\qquad \text{with } k = 0 \text{ and } n = j = 1 \text{ if } t \in]0, t_0], \\ \{{}_M^t\sigma\}_n = \{\sigma_1, \ldots, \sigma_n\} = \{0, \sigma(t_0), \ldots, {}_R^t\sigma\}_n. \end{array}\right.$$

5) Existence of a *non-restrictive neutral initial state* defined by

$$W(O) = \infty, \quad W(O_+) = 0, \quad \omega(O) = 1, \quad \Delta_0^{0+}\sigma = \Delta_0^{0+}\varepsilon = \sigma(O) = O.$$

It is restored by the fundamental cyclic path, independently of the previous paths.

2.2. Toward the tensorial constitutive pattern

Due to Eqs. (2.5) and (2.6), it is interesting to take as a starting point

$$\frac{\partial}{\partial t}\,{}_R^t\cdot S^i{}_j = 0 \tag{2.11}$$

and

$$\left|\begin{array}{l} \dfrac{\partial S^i{}_j}{\partial t} = a_0\delta^i{}_j + a_1 D^i{}_j + a_2 \Delta_R^t \overline{S}^i{}_j, \\ a_0 = \lambda_0 \mathrm{I}_D, \quad a_1 = 2\mu_0, \quad a_2 = \beta_4 \overline{M}, \quad \beta_4 = \dfrac{-\mu}{(\omega S_0)^2}, \end{array}\right. \tag{2.12}$$

respectively. The associated second invariant form is then obtained from Eq. (2.11) and from

$$\frac{\partial \overline{S}^i{}_j}{\partial t} = a_1 \overline{D}^i{}_j + a_2 \Delta_R^t \overline{S}^i{}_j$$

by contraction with $\Delta_R^t \overline{S}^j{}_i$. This yields

$$\dot{\overline{\mathrm{II}}}_{\overline{\Delta S}} = [2\mu + \beta_4 2\overline{\mathrm{II}}_{\overline{\Delta S}}]\overline{M} = \left[2\mu + \frac{-\mu}{(\omega S_0)^2} 2\overline{\mathrm{II}}_{\overline{\Delta S}}\right]\overline{M} = 2\mu\left[1 - \frac{2\overline{\mathrm{II}}_{\overline{\Delta S}}}{(\omega S_0)^2}\right]\overline{M}$$

which is indeed similar to Eq. (2.6). From Eqs. (2.9), and using the condition $\overline{\Phi} = \overline{M}$ (following Eqs. (2.7)), it is possible to perform the integration along the first loading path ($\omega = 1$). One obtains

$$Q_s^2 = Q_0^2\left[1 - \exp\left(-\frac{\mu W}{S_0^2}\right)\right], \quad W = \frac{-S_0^2}{\mu}\ln\left[1 - \frac{Q_s^2}{Q_0^2}\right], \quad Q_0 = \sqrt{2}S_0. \tag{2.13}$$

Consequently, the possible evaluations in a deviatoric plane are, as required, bounded by von Mises circle of radius Q_0. However, caution is obviously needed regarding the first

unloading branch, since the algorithmic coincidence of the help function level may occur for stress points located beyond the von Mises circle (Fig. 3).

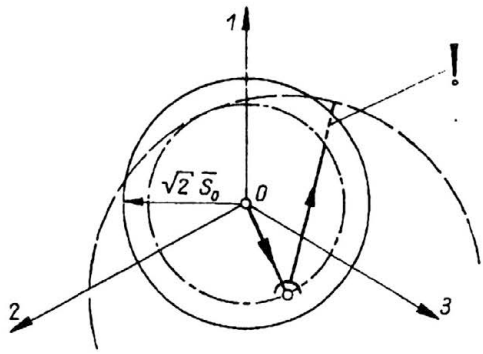

FIG. 3. R^2 example in a deviatoric plane.– – – – – – Mises yield locus,
– · – · – equivalent level of the help function W,
– – – – possible unloading to return on the W first loading level.

Consequently, the yield value S_0 must be replaced by a functional Z_0 taking into account a notation of *orientation* (Fig. 3) according to the form

$$(2.14)\qquad \left|\begin{array}{l} Z_0 = S_0\cos(\pi-\alpha)\,, \quad \alpha = \varphi_{\Delta s} - \varphi_R\,, \quad \beta_4 = \dfrac{-\mu}{(\omega Z_0)^2}\,, \\ W = \displaystyle\int_{t_R}^{t} \frac{2}{\omega^2}\frac{\overline{M}\,dt}{\omega'(S_0,\varphi_{\Delta s}-\varphi_R)^2}\,, \quad \omega'(S_0,\varphi_{\Delta s}-\varphi_R) = \frac{S_0}{Z_0}\,, \end{array}\right.$$

so that the definition of Z_0 is based on the consideration of *asymptotic states* M_1 and M_2 (Fig 4b) such that $M_1M_2 = 2Z_0 = \omega Z_0 = \omega Q_0(\alpha)$.

The role of asymptotic states such like M_1 and M_2 is usually of importance in thermostatics. Therefore one notices not only that the introduction of an orientation parameter α expressed the trivial discrimination between the one and two-dimensional situations, but also that the role of M_1 and M_2 suggests coming back on this conceptual hinge with the help of the notion of reversible and entirely irreversible paths. The fact is that, in the two-dimensional case, there exist not only infinitesimal quasi-reversible paths to the right of an inversion point, but also the possibility of finite paths quasi-reversible in the sense of

$$\overline{\Phi} = 0 \quad \text{with } \overline{\Phi} = \overline{M} + (\text{ "orientation"-dependent rate } : ODR)$$

where the *ODR* remains to be defined.

Therefore it is necessary to come back to the definition (2.12) in order to obtain $\dot{\overline{\Pi}}_{\overline{\Delta S}}$ under the new form

$$\dot{\overline{\Pi}}_{\overline{\Delta S}} = (2\mu + \beta_4 2\overline{\Pi}_{\overline{\Delta S}})\overline{\Phi}\,, \quad \overline{\Phi} = \overline{M} + ODR$$

making use of Eqs. (2.14) to define β_4 and discriminating *radial paths* along which $\overline{\Phi} = \overline{M}$ or $\dot{\overline{\Pi}}_{\overline{\Delta S}}$ are maximum from *neutral paths* along which $\overline{\Phi}$ is zero, so that *any path may be split up into a set of infinitesimal paths alternately radial and neutral.*

But,on the other hand, we notice from Eqs. (2.13) that during the first loading the neutral paths are the circles centered at the origin: then, the radial-neutral discrimination

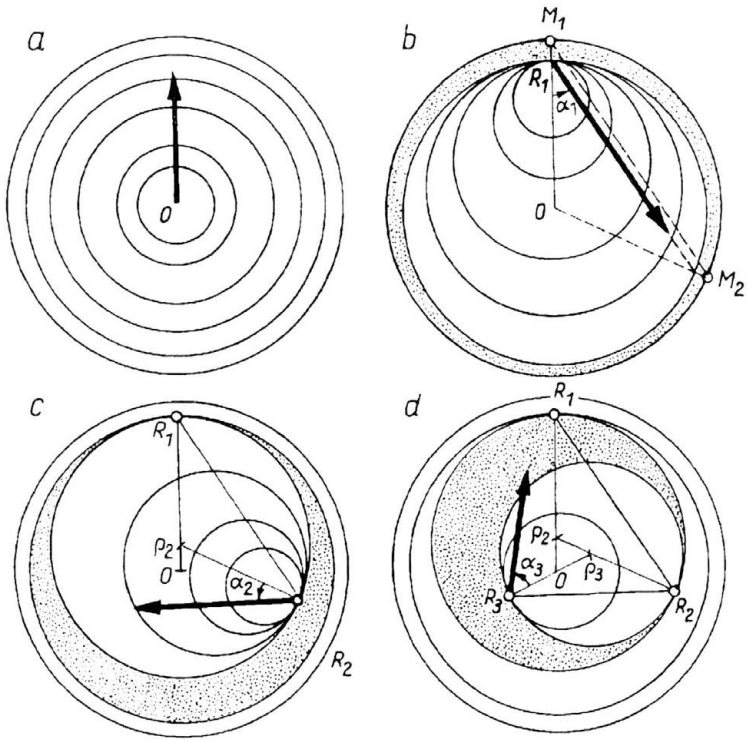

FIG. 4. Location of the locus during the first loading (a) and after 3 reversals of the loading (b, c, d). The shaded zones are not accessible without coincidence of the W levels.

appears compatible with the yield surface notion (Fig. 4a) providing that one makes use of a simple assumption consisting of *the similarity of the neutral paths with respect to the yield locus*.

Consequently, the onset of the first unloading gives rise to a *discontinuous process* obtained through the sliding of the neutral locus and giving, to the right of the inversion, a family of loci without intersections (Fig. 4a, b, c, d).

Therefore, as Π has been previously supposed to be constant along the *finite* branch of a cycle, the assumption is then made that *the family of neutral paths at* t_{R+} *is fixed on the whole of the unloading path*. The crucial invariance is no more that of Π or ${}_R^t\sigma$ but that of ${}_R^t\sigma$ *only*: Π and ${}_R^t\sigma$ are no more "identical" ($D = \pm 1$) as in the one-dimensional case. The same situation arises with respect to $\overline{\Phi}$ and $\overline{M}$: $\overline{\Phi}$ *is no more identical to* $\overline{M}$ as in the one-dimensional case (Eq. (2.7)). However, the discrete memory process remains founded on information sets regarding only the *previous reference state*: the basic form of the pure hysteresis algorithm $(2.10)_3$ can be easily enlarged to the tensorial case following the sketch of Fig. 4 (point iii, Sect. 2.3 below).

2.3. The tensorial pattern

i) Owing to the notions introduced above (Subsects. 2.1 and 2.2), the following assumptions are introduced:

1) non-rotational homogeneous kinematics with fixed principal directions;

2) uncoupled isotropic and deviatoric properties;
3) linearity with respect to D;
4) quasi-reversibility to the right of an inversion point;
5) similarity of the radial paths with respects to the first loading path;
6) similarity of the neutral paths with respect to the yield locus;
7) splitting up of any path into infinitesimal radial-neutral series of

$$\text{radial paths such as } \dot{\varphi}_\Delta = 0 \quad \text{and } \overline{\Phi} \equiv \overline{M},$$

$$\text{neutral paths such as } \dot{\varphi}_\Delta \neq 0 \quad \text{and } \overline{\Phi} \equiv 0.$$

Owing to Eqs. (2.12), the condition 3 above may be satisfied with

$$a_0 = \beta_0 \mathrm{I}_D + \beta_3 \overline{M} + \beta_5 \overline{N}, \quad a_1 = \beta_1, \quad a_2 = \beta_2 \mathrm{I}_D + \beta_4 \overline{M} + \beta_6 \overline{N}.$$

But the condition 2 is strongly restrictive on β_2, β_3 and β_5. One considers

$$\left| \begin{array}{l} a_0 = \beta_0 I_D, \quad \beta_0 = \lambda_0, \quad \beta_3 = \beta_5 = 0, \\ a_1 = 2\mu_0, \\ a_2 = \beta_4 \overline{M} + \beta_6 \overline{N}, \quad \beta_2 = 0. \end{array} \right.$$

Therefore, the second and third invariant forms associated with (2.12)

$$\dot{\overline{\mathrm{II}}}_{\overline{\Delta S}} = a_1 \overline{M} + a_2 \overline{N}, \quad \dot{\overline{\mathrm{III}}}_{\overline{\Delta S}} = a_1 \overline{N} + a_2 3\overline{\mathrm{III}}_{\overline{\Delta S}}$$

become the following basic forms:

$$\begin{aligned} \dot{\overline{\mathrm{II}}}_{\overline{\Delta S}} &= (2\mu + 2\beta_4 \overline{\mathrm{II}}_{\overline{\Delta S}}) \overline{M} + 2\beta_6 \overline{\mathrm{II}}_{\overline{\Delta S}} \overline{N}, \\ \dot{\overline{\mathrm{III}}}_{\overline{\Delta S}} &= 3\beta_4 \overline{\mathrm{III}}_{\overline{\Delta S}} \overline{M} + (2\mu + 3\beta_6 \overline{\mathrm{III}}_{\overline{\Delta S}}) \overline{N}. \end{aligned} \tag{2.15}$$

Moreover, it is worth to notice the formula

$$a_1 \left(\frac{\overline{M}}{2\overline{\mathrm{II}}_{\overline{\Delta S}}} - \frac{\overline{N}}{3\overline{\mathrm{II}}_{\overline{\Delta S}}} \right) = \frac{\dot{\overline{\mathrm{II}}}_{\overline{\Delta S}}}{2\overline{\mathrm{II}}_{\overline{\Delta S}}} - \frac{\dot{\overline{\mathrm{III}}}_{\overline{\Delta S}}}{3\overline{\mathrm{III}}_{\overline{\Delta S}}} = \mathrm{tg}\, 3\varphi_{\Delta s} \dot{\varphi}_{\Delta s}, \tag{2.16}$$

which holds even when condition 2 is not required (Sect. 3 below).

It is now possible to define the scheme with the help of the studies of radial and neutral paths submitted to the similarity rules 5 and 6.

ii) Regarding the radial paths, one gives only short hint and the results. The hint is implied in Eqs. (2.13): it is not only convenient but also relevant to study the stress-energy functional *instead* of the stress-strain functional [2]. With the aid of Eqs. (2.14) and (2.15), one obtains

$$\beta_4 = \frac{-2\mu_0}{[\omega Q_0 \omega'(\omega, \alpha)]^2}, \quad \beta_6 = 0, \quad W = \int_{t_R}^{t} \frac{2}{(\omega\omega')^2} \overline{M}\, d\tau. \tag{2.17}$$

This result gives the required three-dimensional enlargement of Eq. (2.6). Moreover, it is possible to make the same analysis on a generalized form of Eq. (2.6):

$$\frac{\partial \sigma}{\partial t} = G_0 \left(1 - \frac{(\Delta_R^t \sigma)^2}{(\omega S_0)^c (\Delta_R^t \sigma)^{2-c}} \right) \frac{\partial \varepsilon}{\partial t}, \quad c > 0.$$

The result is then

$$\beta_4 = -\frac{2\mu_0}{[\omega Q_0 \omega'(\omega, \alpha)]^c Q_{\Delta s}^{2-c}}.$$

Regarding the neutral paths, it is worth to provide a rather self-contained introduction. The starting point is to express the fourth assumption of point i) by:

$$\frac{\partial}{\partial t}\overline{\Delta_R^t S^i}_j = 2\mu \overline{D^i}_j\,, \qquad \dot{\overline{\mathrm{II}}}_{\overline{\Delta S}} = 2\mu \overline{M}\,. \tag{2.18}$$

Along a general path, it is then possible to consider the deviatoric scheme under a modified form

$$\left|\begin{array}{l} \dfrac{\partial}{\partial t}\overline{\Delta_R^t S^i}_j = 2\mu \overline{D^i}_j + \beta_4' \overline{\Phi}\,\overline{\Delta_R^t S^i}_j\,, \\ \overline{\Phi} = \overline{M} + \gamma_4 \dot{\varphi}_{\Delta s} \end{array}\right. \tag{2.19}$$

on condition that

$$\beta_4' \overline{\Phi} \equiv \beta_4 \overline{M} + \beta_6 \overline{N}\,.$$

This is possible thanks to Eq. (2.16) which gives firstly

$$\overline{\Phi} = \overline{M} + \gamma_4 \frac{2\mu}{\operatorname{tg} 3\varphi_{\Delta s}} \left(\frac{\overline{M}}{2\overline{\mathrm{II}}_{\overline{\Delta S}}} - \frac{\overline{N}}{3\overline{\mathrm{III}}_{\overline{\Delta S}}} \right),$$

and secondly

$$\beta_4 = \beta_4' \left(1 + \frac{2\mu}{2\overline{\mathrm{II}}_{\overline{\Delta S}}} \operatorname{cotg} 3\varphi_{\Delta s} \gamma_4 \right), \qquad \beta_6 = -\beta_4' \frac{2\mu}{3\overline{\mathrm{III}}_{\overline{\Delta S}}} \operatorname{cotg} 3\varphi_{\Delta s} \gamma_4$$

as the result of the identification.

The factor γ_4 remains to be defined using the equation

$$\dot{Q}_{\Delta s} = -\operatorname{tg}(\varphi_{\Delta s} - \varphi_{pR}) Q_{\Delta s} \dot{\varphi}_{\Delta s}$$

of the neutral locus. This equation may be written in the form

$$\dot{\overline{\mathrm{II}}}_{\overline{\Delta S}} = -A \overline{\mathrm{II}}_{\overline{\Delta S}} \dot{\varphi}_{\Delta s}\,, \qquad A = 2 \operatorname{tg}(\varphi_{\Delta s} - \varphi_{\varrho R})$$

so that, from the definition (2.18), one obtains

$$0 = \overline{M} - \frac{\dot{\overline{\mathrm{II}}}_{\overline{\Delta S}}}{2\mu} = \overline{M} + A \frac{\overline{\mathrm{II}}_{\overline{\Delta S}}}{2\mu} \dot{\varphi}_{\Delta s}$$

and

$$\gamma_4 = \frac{A \overline{\mathrm{II}}_{\overline{\Delta S}}}{2\mu} = \frac{\overline{\mathrm{II}}_{\overline{\Delta S}} \operatorname{tg}(\varphi_{\Delta s} - \varphi_{\varrho R})}{\mu}\,. \tag{2.20}$$

iii) The generalization of the pure hysteresis algorithm is immediately obtained by introducing the set of phase $\varphi_{\varrho R}$ of the φ_R set of points (Fig. 4):

$$\{\varphi_{\varrho R}\}_n = \{0, \varphi(t_0), \ldots\}_n\,,$$

which is ordered by following the increasing values of the parameter evolution. The possibility of coincidence of the help function levels without closing a cycle is taken into account with a modification of $\mathcal{A}_c$ according to

$$\mathcal{A}_c : \left|\begin{array}{lll} \overline{S}(t) \stackrel{?}{=} \overline{S}_{n-1} & \text{yes} \xrightarrow[\text{of a cycle}]{\text{closing}} & \mathcal{A}_c = \mathcal{A}_c^2\,, \\ & \text{no} \xrightarrow[\text{of } W \text{ level}]{\text{coincidence}} & \mathcal{A}_c = \mathcal{A}_c^1\,, \end{array}\right.$$

$$\mathcal{A}_c^i \Rightarrow \begin{vmatrix} \omega = 2, & k = k, & \alpha = \alpha + 1, & n = n - i, \\ {}^t_R S = S_n, & {}^t_R W = W_n, & \varphi_{\varrho R} = \varphi_n. \end{vmatrix}$$

The generalization of the intrinsic internal heat flux analysis is founded on the quasi-linearity (2.16) from which one obtains the basic form.

$$\overline{\Phi} = Q_D Q_{\Delta s} = \overline{M}$$

along the radial paths. Therefore one considers the basic calorific rate [2]:

$$\overline{C}^{Ra} = \dot{Q}_{\Delta s} \int_{t_R}^{t} Q_D \, d\tau \tag{2.21}$$

to extend Eq. $(2.10)_2$ along these paths. This form is also used when the path is not radial, making use of the splitting $(\dot{Q}^{Ne}_{\Delta s}\, dt, \dot{\varphi}_{\Delta s}\, dt)$, $(\dot{Q}^{Ra}_{\Delta s}\, dt, 0)$ where $\dot{Q}^{Ne}_{\Delta s}$ is deduced from the neutral paths definition

$$Q^{Ne}_{\Delta s} = \text{cste}\, \omega \omega'(\omega, \varphi_{\Delta s} - \varphi_{\varrho R}).$$

One obtains

$$\begin{vmatrix} \overline{C} = (\omega')^2 \Big[\int_{t_R}^{t} \frac{\dot{Q}^{Ra}_{\Delta s}}{\omega'} d\tau \Big] \Big[\int_{t_R}^{t} \frac{Q^{Ra}_D}{\omega'} d\tau \Big], \\ \dot{Q}^{Ra}_{\Delta s} = \dot{Q}_{\Delta s} - \frac{\omega'}{\omega} Q_{\Delta s}, \quad Q^{Ra}_D = \frac{\overline{\Phi}}{Q_{\Delta s}}. \end{vmatrix} \tag{2.22}$$

Several illustrations are introduced in [2] (an example is also recalled in [14]).

3. The scheme of pure hysteresis with coupling effects

3.1. The two-fold coupling effects

The effects of the deviatoric properties—dev(iso) coupling effect—is taken into account with the above recalled pure *hysteresis scheme* implemented with a conical yield surface of circuit cross-section and using a method of *projection* similar to that previously introduced in the variable temperature case in order to describe the shape memory effects [3, 5] and [7].

The effect of the deviatoric stress invariant Q_s on the volume variations (iso—(dev) coupling effects) is described by following the pattern (1.1).

3.2. From the definition of $Q_{\lim}(p)$ to the definitions of $\mu(p)$ and $\lambda(p)$

Experiments show that it is relevent to choose the ratio $\mu/Q_{\lim}$ in a pressure-independent way ([12] § D, Fig. V.3 to V.6 page 91). Consequently, the simplest reversible rate, of $(3\lambda + 2\mu)I_D$ type, leads us to consider

$$\frac{\alpha_1}{2} = \mu(\varphi, p) = \mu_0 \left(1 - \frac{p}{p_0}\right) = \mu(p) \tag{3.1}$$

owing to the condition of conical yield surfaces

$$Q_{\lim}(\varphi, p) = Q_0 \left(1 - \frac{p}{p_0}\right) = Q_{\lim}(p). \tag{3.2}$$

To remain simple it is necessary to consider also

$$\alpha_0 = \lambda(\varphi, p) = \lambda_0 \left(1 - \frac{p}{p_0}\right) = \lambda(p) . \tag{3.3}$$

Consequently, under purely hydrostatic loading, the scheme is

$$\dot{\mathrm{I}}_{\Delta s} = \left(1 - \frac{p}{p_0}\right)(3\lambda_0 + 2\mu_0)\mathrm{I}_D = (3\alpha_0 + \alpha_1)\mathrm{I}_D .$$

For an isotropic relative deformation $(1 + K)$ of the initial unit cubic element

$$V(t) = \sqrt{g} = J^3 , \quad \ln\sqrt{g} = 3\ln J \quad \text{with } J = 1 + K$$

and

$$3\dot{p} = \left(1 - \frac{p}{p_0}\right)[3\lambda_0 + 2\mu_0)\frac{\dot{V}}{V}$$

so that

$$1 = V\left(1 - \frac{p}{p_0}\right)^{\frac{3p_0}{3\lambda_0 + 2\mu_0}} \quad \text{or} \quad 0 = \ln\sqrt{g} + K_0 \ln\left(1 - \frac{p}{p_0}\right)$$

for p versus V or p versus $\ln\sqrt{g}$ diagrams, respectively.

In fact, experiments are suggesting rather some $(\Delta V/V)^n$ type of scheme ($n \simeq 3/2$) and, moreover, hysteresis effects are obvious (see footnote([1])). However, the challenge of this paper does not imply to define a sophisticated, purely hydrostatic scheme.

The aim of the analysis is indeed to obtain first, *a variable dilatation* under rectilinear *first loading paths* of various given Q_s/I_s ratios and, secondly, to obtain the *compaction effect directly to the right of an inversion point.*

The first requirement is obtained with a remarkable straightforward approach, as shown by one of the authors. The role of $\overline{\Phi}$, and consequently of $\overline{M}$, being indeed of an outstanding importance, it is necessary to extend the definition of $\overline{M}$ by introducing a *pressure-dependent mixed invariant* $\overline{M}_p$. But it appears that $\overline{M}_p$ is linked with $\dot{Q}_{\Delta s}$ so that a linear form with respect to $\overline{M}_p$ is also linked with $\dot{Q}_{\Delta s}$, as required to define a link between I_D and $\dot{Q}_{\Delta s}$. Therefore one considers a provisional scheme

$$\dot{\mathrm{I}}_{\Delta s} = (3\alpha_0 + \alpha_1)\mathrm{I}_D + 3\alpha_3'\overline{M}_p , \tag{3.4}$$

where a relevant definition of α_3' may be suggested by *experimental results.*

The second requirement is achieved in an extended form

$$\dot{\mathrm{I}}_{\Delta s} = \alpha_1\mathrm{I}_D + 3\gamma_{12}(\alpha_0\mathrm{I}_D + \alpha_3'\overline{M}_p + \alpha_3''\overline{\Delta_R^t S^i}_j\,\overline{D^j}_i) \tag{3.5}$$

of the previous provisional scheme, where the introduction of $\overline{\Delta_R^t S^i}_j\,\overline{D^j}_i$ is interesting due to its always non negative value. However, the definition is not as straightforward as that of the provisional scheme and is introduced at the very end of the analysis (Sect. 3.6).

3.3. Definition of the functionals ${}_R^t S_p$, $\Delta_R^t S_p$, $\overline{M}_p$ and $\overline{\Phi}$

Regarding $\overline{M}_p$, the first step of the approach is to extend the neutral path notion to the conical case under consideration (Fig. 5) and to use once more the splitting principle with three (and no longer two) types of infinitesimal paths: radial (φ and p constant), neutral with p constant, neutral with φ constant (Fig. 5).

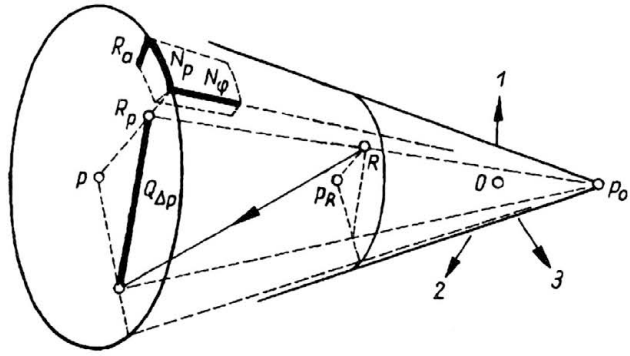

FIG. 5. Three-dimensional splitting up of a path and definition of $Q_{\Delta p}$ (of conical type).

The second step consists in extending the discrete memory condition to the pressure-dependent case and in defining the associated compatible notions regarding the algorithm. Owing to the conical assumption, one considers (Fig. 5)

$$(3.6) \qquad {}^t_R S_p \overset{\text{def}}{=} p\mathbf{1} + \frac{p_0 - p}{p_0 - p_R} {}^t_R \overline{S},$$

and the associated role of a modified W functional

$$(3.7) \qquad \dot{W}_p \overset{\text{def}}{=} \frac{\dot{W}}{\left(1 - \dfrac{p}{p_0}\right)}.$$

The third point of the analysis leads to the $\overline{M}_p$ definition. It is obtained by maintaining

$$(3.8) \qquad \frac{\partial}{\partial t} \overline{S}^i{}_j = 2\mu \overline{D}^i{}_j$$

to define neutral paths and using this form to express $\dot{\overline{\Pi}}_{\overline{\Delta S}}$ by two different methods in order to link $\dot{Q}_{\Delta p}$ and $\overline{M}_p$ along a neutral path of constant phase.

On the one hand, if

$$Q_s = \tilde{Q}_0 \left(1 - \frac{p}{p_0}\right),$$

one obtains

$$\dot{Q}_s = \frac{-\dot{p} Q_s}{(p_0 - p)},$$

and for $Q_{\Delta p}$ one has also (Fig. 5)

$$Q_{\Delta p} \dot{Q}_{\Delta p} = \dot{\overline{\Pi}}_{\Delta p} = -\dot{p} \frac{Q^2_{\Delta p}}{(p_0 - p)}, \qquad Q^2_{\Delta p} = \overline{\Delta {}^t_R S^i_{pj}}\, \overline{\Delta {}^t_R S^j_{pi}}.$$

On the other hand, the definition (3.6) of ${}^t_R S_p$ gives

$$\overline{\Delta {}^t_R S_p} = \overline{S} - {}^t_R \overline{S}_p = \overline{S} - \frac{p_0 - p}{p_0 - p_R} {}^t_R \overline{S},$$

so that

$$\dot{\overline{\Delta {}^t_R S_p}} = \dot{\overline{S}} + \frac{\dot{p}}{p_0 - p_R} {}^t_R \overline{S}.$$

Using Eq. (3.8) one has

$$\frac{\partial}{\partial t}(\overline{\Delta_R^t S_p})^i{}_j = 2\mu \overline{D}^i{}_j + \frac{\dot{p}}{p_0 - p_R} {}_R^t\overline{S}^i{}_j$$

and, contracting with $(\overline{\Delta_R^t S_p})^j{}_i$, one obtains

$$\dot{\overline{\Pi}}_{\Delta p} = 2\mu \overline{M}_p + \frac{\dot{p}}{p_0 - p} \overline{K}_p$$

with the required definitions

$$\overline{M}_p = (\overline{\Delta_R^t S_p})^j{}_i \overline{D}^i{}_j , \qquad \overline{K}_p = {}_R^t\overline{S}^i{}_j (\overline{\Delta_R^t S_p})^j{}_i .$$

Consequently,

$$0 = \overline{M}_p + \frac{1}{2\mu} \frac{Q_{\Delta p}^2 + \overline{K}_p}{p_0 - p} \dot{p} ,$$

and there remains only to introduce the fundamental form

$$\overline{\Phi} = \overline{M}_p + \gamma_4 \dot{\varphi}_{\Delta s} + \Gamma_4 \dot{p}$$

and the previous scheme

$$\dot{\overline{S}} = 2\mu \overline{D} + \beta_4 \overline{\Phi} \overline{\Delta S}$$

to obtain

$$\Gamma_4 = \frac{Q_{\Delta p}^2 + \overline{K}_p}{2\mu(p_0 - p)}$$

by identification along the neutral paths under consideration.

3.4. Definition of the scalar functional α_3 giving the basic term $\alpha_3 \overline{M}_p$

The factor α_3' remains to be defined. Let $\mathrm{I}_{D\,\mathrm{lim}}$ denote the limit of the value of I_D associated with the plastic yield limit of the first loading where $\dot{\mathrm{I}}_{\Delta s}$ tends toward zero. One obtains

$$\mathrm{I}_{D\,\mathrm{lim}} = \frac{-3\alpha'_{3\,\mathrm{lim}} \overline{M}_{p\,\mathrm{lim}}}{3\alpha_0 + \alpha_1} = \frac{-3\alpha'_{3\,\mathrm{lim}} \overline{M}_{p\,\mathrm{lim}}}{(3\tilde{\lambda}_0 + 2\tilde{\mu}_0)\left(1 - \dfrac{p}{p_0}\right)}$$

and

$$\overline{M}_{p\,\mathrm{lim}} = Q_{\mathrm{lim}} \| D_{\mathrm{lim}} \| = \left(1 - \frac{p}{p_0}\right) Q_0 \| D_{\mathrm{lim}} \| ,$$

so that

$$\frac{\mathrm{I}_{D\,\mathrm{lim}}}{\| D_{\mathrm{lim}} \|} = \frac{3Q_0}{3\lambda_0 + 2\mu_0} \alpha'_{3\,\mathrm{lim}} .$$

Then the definition results in the use of a previously proposed form, $\exp(-\gamma Q)$, of the ratio $\mathrm{I}_{D\,\mathrm{lim}} / \| D_{\mathrm{lim}} \|$: such a form has been recognized as qualitatively compatible with the experimental results ([12]). Consequently, introducing the two parameters γ_0 and E_0, one considers

$$\alpha'_{3\,\mathrm{lim}} = -\frac{3\lambda_0 + 2\mu_0}{3Q_0} E_0 \exp\left(-\gamma_0 \frac{Q_{\mathrm{lim}}}{Q_0}\right)$$

and α'_3 is simply defined as

$$\alpha'_3 = -\alpha'_{3\,\mathrm{lim}} Q_{R\Delta}\,, \tag{3.9}$$

where the "reduced deviatoric" invariant $Q_{R\Delta}$ is

$$Q_{R\Delta} = \frac{Q_{\Delta p}}{\omega Q_0 \left(1 - \dfrac{p}{p_0}\right)} = \frac{Q_{\Delta p}}{\omega Q_{\mathrm{lim}}(p)}\,.$$

Thus, the description of the first loading ($\omega = 1$) is given by the provisional scheme

$$\dot{\mathrm{I}}_{\Delta s} = (\alpha_1 + 3\alpha_0)\mathrm{I}_D + \frac{3\lambda_0 + 2\mu_0}{Q_0} E_0 \exp\left(-\gamma_0 \frac{Q_{\mathrm{lim}}}{Q_0}\right) Q_{R\Delta} \overline{M}_p\,.$$

3.5. The cyclic case and the final form of the isotropic part of the scheme

The cyclic case ($\omega = 2$) must still be dealt with. It is convenient to divide the analysis into the following three parts.

i) First, it is clear that the use of the provisional scheme (3.4) in the cyclic case is doubtful owing to the fact that $\overline{M}_p$ is zero at the onset of each cycle branch, so that the rate $(3\lambda + 2\mu)\,\mathrm{I}_D$ is the only one able to balance the hydrostatic stress rate. In spite of this disturbing situation, it is easy to obtain, in the case of *large cycles*, the required compaction-extension effect already obtained above. This may be achived only with the help of a new simple definition of α'_3

$$\alpha'_3 = \frac{-\alpha'_{3\,\mathrm{lim}}}{\omega}[Q_{R\Delta} - \beta_3(\omega - 1)(1 - Q_{R\Delta})]$$

instead of Eq. (3.9). In this definition, a new physical parameter β_3 is introduced.

ii) The second part of the analysis is devoted to the definition of a better balance of the hydrostatic rate introducing a non-vanishing term of constant sign at the onset of the branch. A simple choice is that of the power $\overline{S}\,\overline{D}$ and, consequently, one adds a $\alpha''_3\,\mathrm{tr}\,\overline{S}\,\overline{D}$ term in the scheme, with

$$\alpha''_3 = -\frac{\alpha'_{3\,\mathrm{lim}}}{\omega}\beta'_3(\omega - 1)(1 - Q_{R\Delta})\,. \tag{3.10}$$

The resulting scheme is relevant for the case of large cycles: β_3 allows us to obtain the dilatation and β'_3 gives the required compaction effect at the onset of an extension (Fig. 7). But the use of $\overline{S}\,\overline{D}$ term gives rise to an irrelevant behaviour in the case of small cycles, since a change of sign of $\mathrm{tr}\,S \cdot D$ is possible.

iii) An alternative choice consists in the use of the invariant $\Delta\overline{S}\,\overline{D}$ which is of constant sign but is unfortunately zero at the onset of a branch so that it must be divided by another vanishing form. Consequently one considers

$$\alpha''_3 = \frac{\omega Q_{\mathrm{lim}}}{Q_{\Delta s}}\,,$$

α''_3 given by Eq. (3.10).

The only inconvenience of the new $\alpha''_3\,\mathrm{tr}\,\Delta\overline{S}\,\overline{D}$ term is that it requires a special alternative form: at the onset of the branch $(\mathrm{tr}\,\Delta\overline{S}\,\overline{D})/Q_{R\Delta}$ must be replaced by $(\mathrm{tr}\,\dot{\overline{S}}\,\overline{D})/Q_{\dot{s}}$.

Finally, it is necessary to define the γ_{12} coefficient of Eq. (3.5),

$$\gamma_{12} = 1 + (\omega - 1)\gamma_1 \exp(-\gamma_2 Q_{R\Delta}) .$$

Consequently, in the case $\omega = 2$, the scheme suggested by Eq. (3.5) is

$$\dot{\mathrm{I}}_{\Delta s} = \alpha_1 \mathrm{I}_D + 3(1 = \gamma_1 \exp(-\gamma_2 Q_{R\Delta})) \left\{ \alpha_0 \mathrm{I}_D + \frac{3\lambda_0 + 2\mu_0}{6Q_0} E_0 \exp\left(\frac{-\gamma_0 Q_{\lim}}{Q_0}\right) \right.$$
$$\left. \times \left((Q_{R\Delta} - \beta_3(1 - Q_{R\Delta}))\overline{M}_p + \beta_3'(1 - Q_{R\Delta}) \frac{2Q_{\lim}}{Q_{\Delta s}} \operatorname{tr} \overline{\Delta S}\, \overline{D} \right) \right\} ,$$

where the physical parameters are not only μ_0, λ_0, Q_0, p_0, γ_0 and E_0 but also γ_1, γ_2, β_3 and β_3'. Like β_3 and β_3', the interesting values of parameters γ_1 and γ_2 are of the order of a few units.

The cases $\omega = 1$ and $\omega = 2$ are included in the form

$$\dot{\mathrm{I}}_{\Delta s} = \alpha_1 \mathrm{I}_D + 3(1 + \gamma_1(\omega - 1)\exp(-\gamma_2 Q_{R\Delta})) \left\{ \alpha_0 \mathrm{I}_D + \frac{3\lambda_0 + 2\mu_0}{3\omega Q_0} E_0 \exp\left(\frac{-\gamma_0 Q_{\lim}}{Q_0}\right) \right.$$
$$\left. \times \left((Q_{R\Delta} - \beta_3(\omega - 1)(1 - Q_{R\Delta}))\overline{M}_p + \beta_3'(\omega - 1)(1 - Q_{R\Delta}) \frac{\omega Q_{\lim}}{Q_{\Delta s}} \operatorname{tr} \overline{\Delta S D} \right) \right\} ,$$

where the basic notation may be summed up by

$$\left| \begin{array}{l} Q_{\lim} = Q_0 \left(1 - \dfrac{p}{p_0}\right) , \quad Q_{R\Delta} = \dfrac{Q_{\Delta p}}{\omega Q_{\lim}} , \quad Q^2_{\Delta p} = \overline{\Delta^t_R S_p{}^j{}_i \Delta^t_R S_p{}^j{}_i} , \\ Q^2_{\Delta s} = \overline{\Delta^t_R S^i{}_j \Delta^t_R S^j{}_i} , \quad \alpha_1 = 2\mu = 2\mu_0 \left(1 - \dfrac{p}{p_0}\right) , \quad \alpha_0 = \lambda = \lambda_0 \left(1 - \dfrac{p}{p_0}\right) . \end{array} \right.$$

The deviatoric part of the scheme is given by Eqs. (2.17), (2.19) and (2.20).

4. Usual axisymmetrical first loading and large cyclic loading

4.1. Axisymmetrical ($\sigma_1 = \sigma_2$) first loading

After the hydrostatic loading from 0 to p_1, ten integrations are performed along rectilinear stress paths; the tilting angle $\psi(\operatorname{tg}\psi = Q_s/(p - p_1))$ of these rectilinear paths with respect to the hydrostatic axis are such as:

$\psi = 30°,\ 50°,\ 60°,$

then $\sigma_1 = \text{cst}$, $I_s = \text{cst}$, $\sigma_3 = \text{cst}$ in compression,

finally $\sigma_1 = \text{cst}$, $I_s = \text{cst}$, $\psi = 70°$, $\sigma_3 = \text{cst}$ in extension.

This scheme appears to be relevant, at least qualitatively, owing to the result obtained (Fig. 6), with the following parameters values:

$$\mu_0 = 12.29\text{MPa}, \quad \lambda_0 = 3\mu_0, \quad Q_0 = 0.35\text{MPa}, \quad p_0 = 0.55\text{MPa}, \quad \gamma_0 = 0.1, \quad E_0 = 0.58.$$

The values of the last two parameters are comparable with those of [12]. One can notice the following points:

the dilatation is not bounded, but may be easily limited if required,

the weak dilatant tendency of path number 10 is due to a path close to the yield surface: the path is indeed tilted 50.77° and the yield surface is tilded at 47.8°.

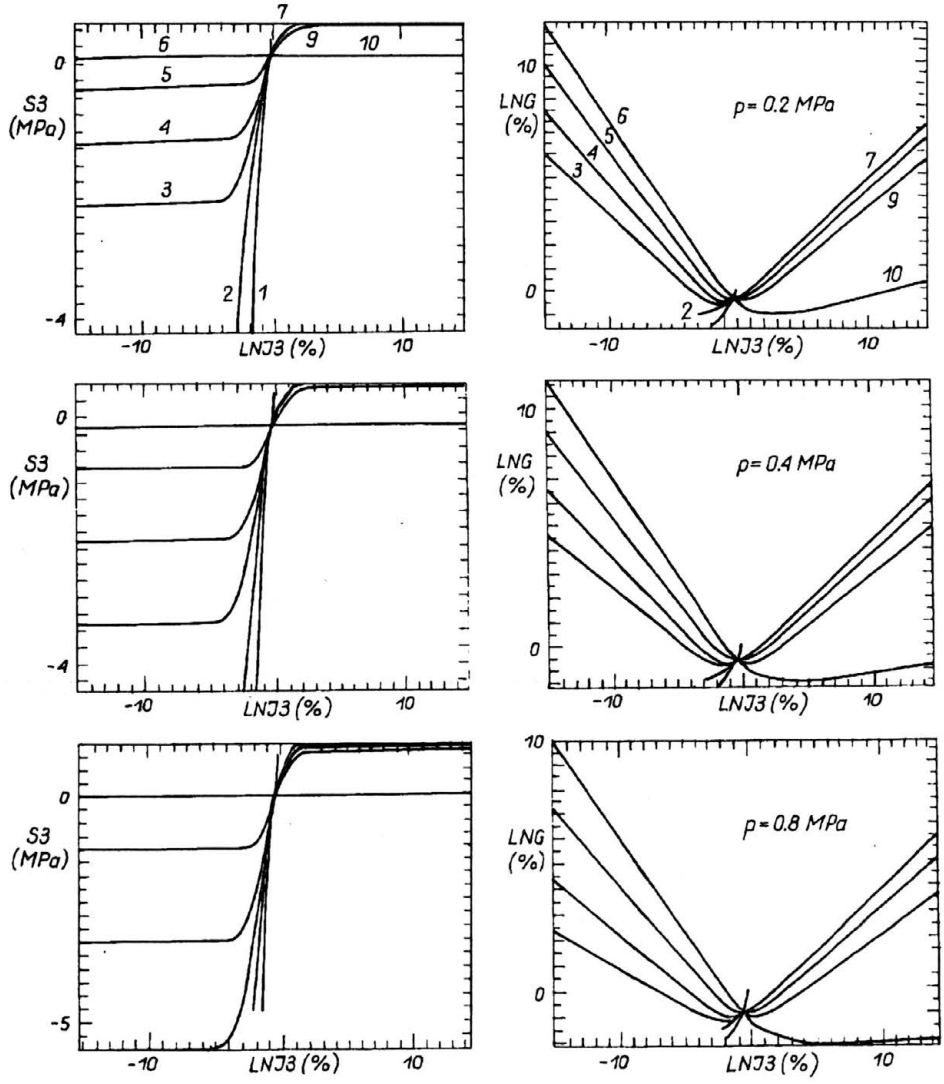

FIG. 6. Axial stress S_3 versus axial deformation $\ln J_3$ ($J_3 = 1 + k_3$) and relative volume variation $\ln \sqrt{g}$ versus $\ln J_3$ (at right) for various rectilinear first loading paths starting from 3 hydrostatic pressures ($p_i = -0.2$ MPa, - 0.4 MPa and - 0.8 MPa). Paths 1 to 6 are in compression (1 to 3 titled at 30, 50, and 60°; 4 biaxial; 5 deviatoric; 6 constant axial stress). Paths 7 to 10 are in extension (7 titled at 70°; 8 deviatoric; 9 biaxial; 10 constant axial stress).

4.2. Large cyclic loading

The usual cyclic biaxial test is performed under controlled strain, both with the first deviatoric loading in the direction of compression and tension (Figs. 7a and b). Using the same values of the physical parameters, a cyclic path in the deviatoric plane ($\Psi = \pi/2$) is also performed (Fig. 7c).

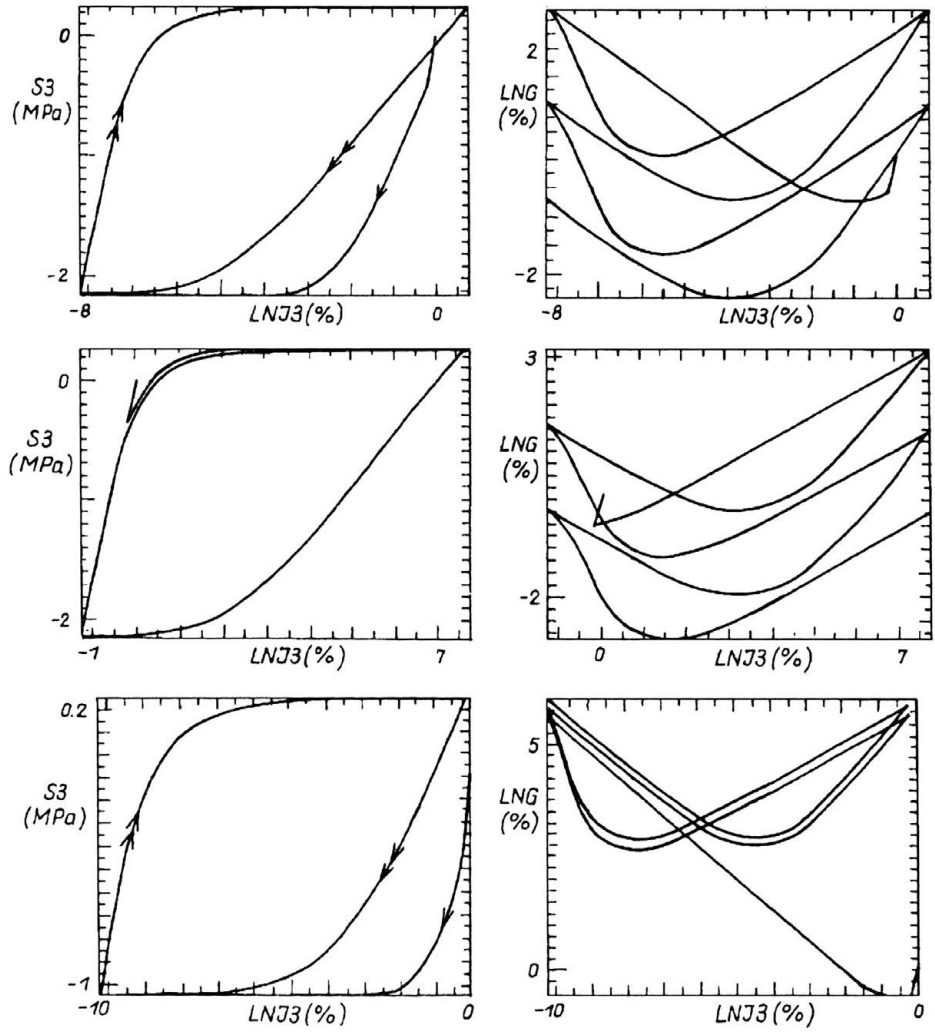

FIG. 7. Cyclic biaxial test (starting with compression or extension) and constant pressure test: $\beta_3 = 10$; $\beta_3' = 4$. Same notations as in Fig. 6.

5. Illustrations regarding the case of small, medium and large cyclic loading

The aim of this paragraph is to illustrate rather extensively the capabilities of the final *coupled* scheme to describe quasi-cycles, *whatever the amplitudes of the cycles may be*, and at least qualitatively in accordance with the deviatoric and volumic properties of sand-like materials.

5.1. Small cycles under specified cyclic strain

The physical parameters μ_0, λ_0, Q_0, p_0, γ_0 and E_0 remain those previously used.

The biaxial compression is specified up to 5% and the cyclic evolution is performed

in the interval [0.04, 0.05]. The illustrations are given with:

a) $\beta_3 = 4$, $\beta_3' = 0.2$, $\gamma_1 = 10$, $\gamma_2 = 5$,

b) $\beta_3 = 4$, $\beta_3' = 0.4$, $\gamma_1 = 10$, $\gamma_2 = 5$,

c) $\beta_3 = 4$, $\beta_3' = 0.4$, $\gamma_1 = 0$, $\gamma_2 = 0$.

The parameter β_3' gives the control of a "symmetrical" peak effect (Fig. 8), and the parameters γ_1 and γ_2 are able to modify the tilting of the cycles in a relevant way.

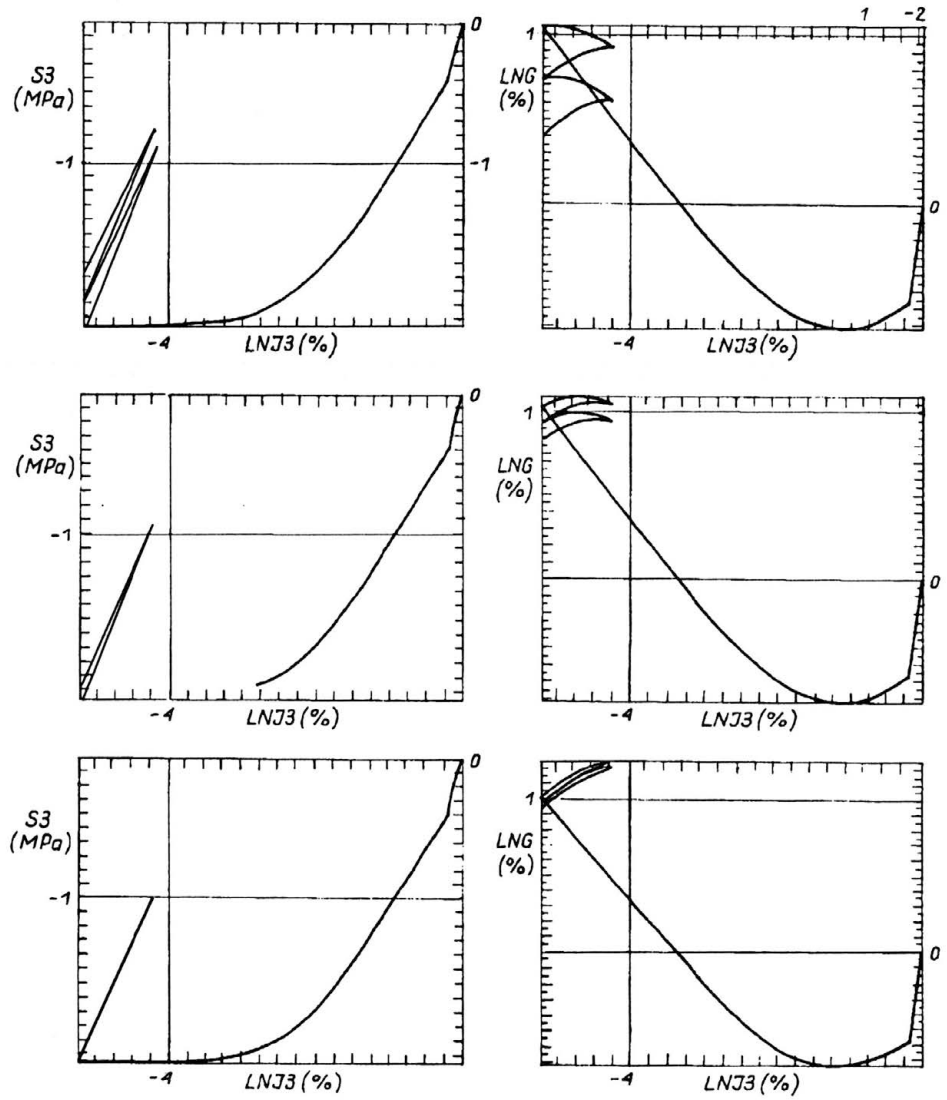

FIG. 8. Strain-controlled small cycles. The parameters $|\beta_3; \beta_3', \gamma_1; \gamma_2|$ are $|4; 0.2; 10; 5|$; $|4; 0.4; 10; 5|$; $|4; 0.4; 0; 0|$ respectively. Same notations as in Figs. 6 and 7.

5.2. Small, medium and large cycles under specified cyclic stress

The cyclic evolutions are now performed under stress control with the following amplitudes 0.7 MPa (small cycles), 1.2 Mpa (medium cycles) and 2.2 MPa (large cycles). The set (γ_1, γ_2 β_3', β_3') of parameters is 2, 5, 6, 0.4 (Fig. 9).

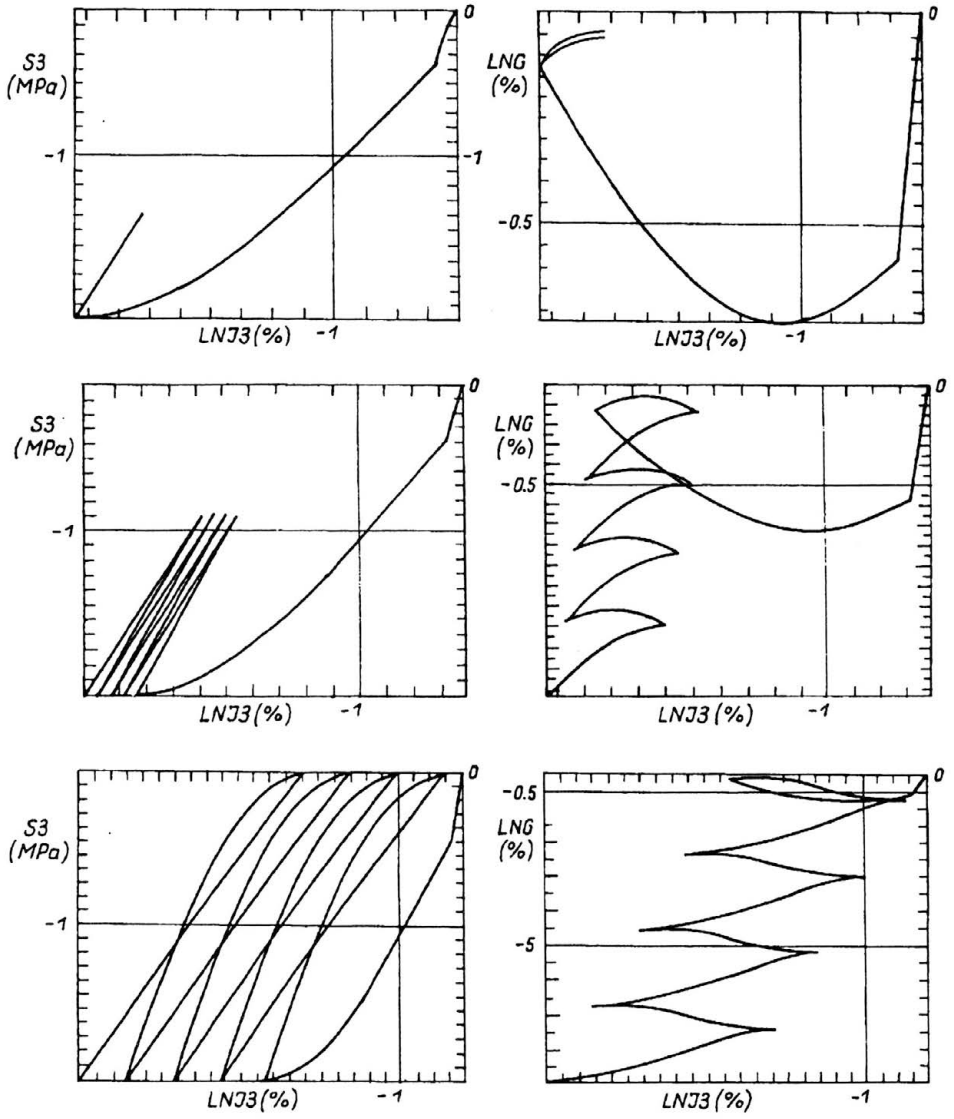

FIG. 9. Stress-controlled small, medium and large cycles.
The set of parameters $|\beta_3; \beta_3'; \gamma_1; \gamma_2|$ is $|6; 0.4; 2; 5|$.
Same notations as in Figs. 6, 7 and 8.

6. Concluding remarks

The clue of the analysis has been obtained through the definition of the functionals ${}^{t}_{R}S_{p}$, $\Delta {}^{t}_{R}S_{p}$, $\overline{M}_{p}$ and $\overline{\Phi}$ (Sect. 3.4). Although the Coulomb yield effects and anisotropic effects have been neglected, the properties of the proposed scheme are interesting regarding questions which are up to now unsolved (point iv of Sect. 1).

It remains to introduce a well founded definition of the preferred reference frames including a consistent generalization of the whole pattern to the anisotropic case. A solution to this problem is from now on outlined.

As soon as this problem will be overcome, it will be possible to go deeply into the study of "Coulomb" effects and "hydrostatic" effects (points v and vi of Sect. 1).

Appendix

The pattern of *pure hysteresis* behaviour and its associated symbolic model are *heuristic when some particular insight is needed for the study of fundamental microscopical processes* based on the *dislocation concept*.

Since a few years it is possible, with the aid of transmission electron microscopy, to observe dislocation movements occurring with the deformation of small samples. For the study of pure hysteresis, the interesting mechanisms are those related to the case of stationary cycles after stabilization of the microstructural phenomena. Under those conditions a notable analogy between gliding microstructural processes and the pure hysteresis symbolic model has been recently established ([4, 13 and 14]).

The simplest case is represented by a *simple dislocation* moving between two parallel walls: the process is analogous to the simplest symbolic model (one spring and one friction

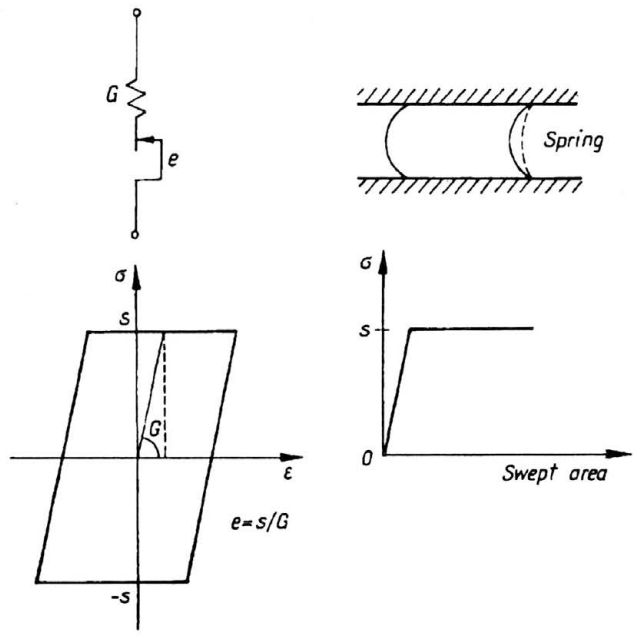

FIG. 10. A microstructural process analogous to the elastic-plastic process of the simplest symbolic model.

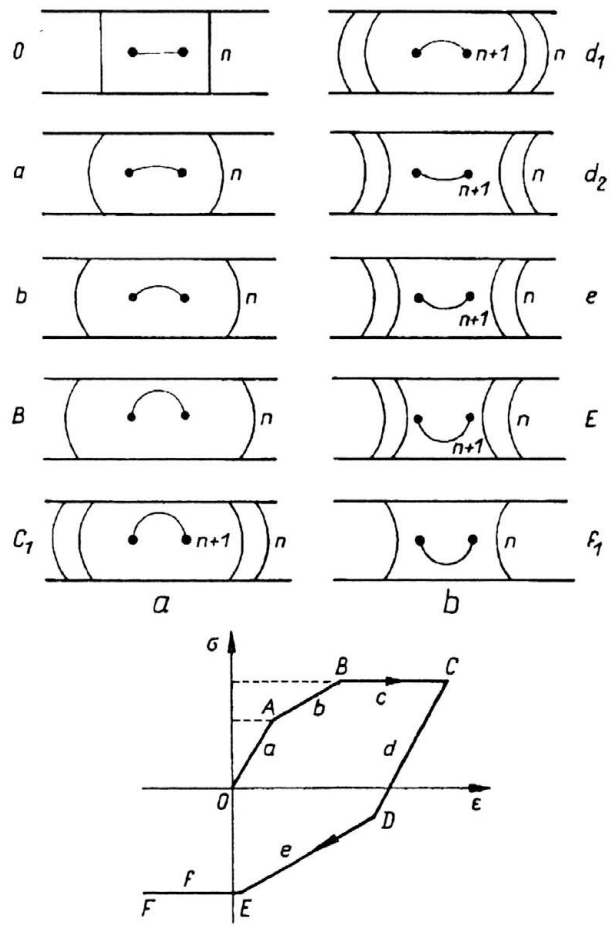

FIG. 11. The Frank-Read process during a cycling loading: a) first loading $OABC$, b) first unloading $CDEF$.

slider associated in series). Under small stress the dislocation will bend reversibly and behaves like the spring. For a characteristic values S_0 of the stress, the *dislocation pinning points will move and drag two segments along the walls*: the behaviour is analogous to that of the friction slider (Fig. 10). The diagram of the stress versus the area swept by the dislocation is of elastic-perfectly plastic type.

When the stress decreases it is necessary for the stress to reach the opposite value $-S_0$, before the pinning points move in the opposite directions. This behaviour is thus really of pure hysteresis type.

A more complex case is the one of a *Frank–Read source* acting between two parallel walls and characterized by two thresholds, S_1 for which the pinning points move and $S_2 > S_1$ for which the source emits a loop (Fig. 11). This case is equivalent to a model with two couples.

During unloading a process of loop absorption may exist (Fig. 12) and has actually been observed.

In a real crystalline material the deformation is the result of the activation of a great

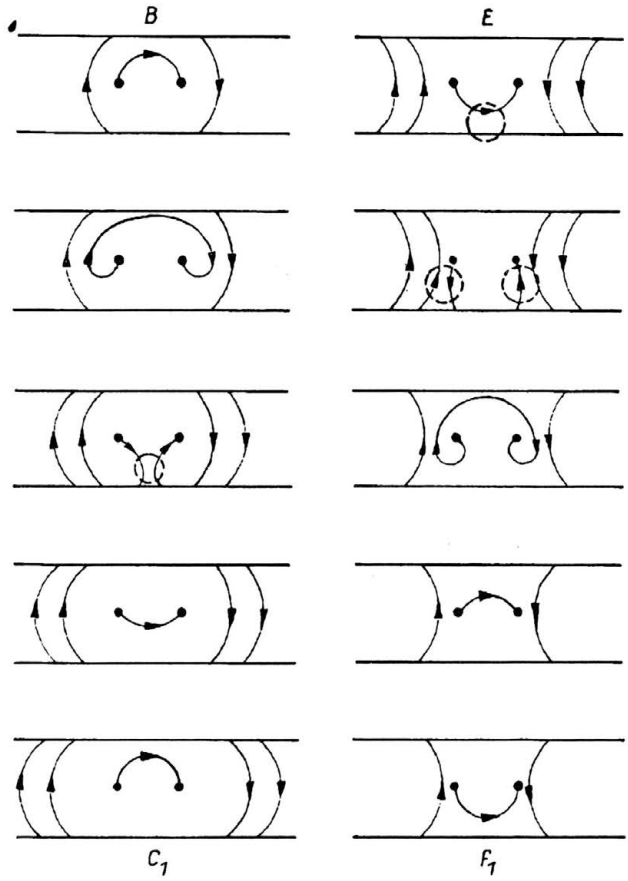

FIG. 12. Process of loop absorption during unloading $CDEF$.

number of elementary mechanisms like the proceeding one. The activation thresholds of these mechanisms are largely and continuously dispersed due to different parameters such as type, characteristic values, orientations with respect to the "external stress", intergranular compatibility, etc.

On the basis of this analogy it is possible to give an evident physical interpretation of the pure hysteresis properties; this is particularly the case of the stress-strain discontinuity obtained by describing a small cycle inside a large cycle. This is also the case for the properties to the right of an inversion point, for the fundamental cyclic loading properties and for the absence of reversible domain of the real crystalline materials ([4, 13] and [14]).

References

1. M. P. LUONG, *Détection par thermographie infrarouge du seuil caractéristique d'un sable cisaillé en vibrations*, Comptes rendus Académie des Sciences à Paris, 295, 87–88, 1982.
2. P. PEGON, *Contribution à l'étude de l'hystérésis élastoplastique*, Thèse, Grenoble 1988.
3. D. FAVIER, *Contribution à l'étude théoretique de l'élastohystérésis à température variable: application aux proprietes de mémoire de forme*, Thèse, Grenoble 1988.

4. A. TOURABI, *Contribution à l'étude de l'hystérésis élastoplastique et de l'écrouissage des métaux et alliages réels*, Thèse, Grenoble 1988.
5. D. FAVIER, P. GUELIN, P. PEGON, A. TOURABI and B. WACK, *Ecrouissages, schémas thermomécaniques et à variables internes: methode de définition utilisant le concept d'hystérésis, pure*, Arch. Mech., 40, 5–6, 611–640, 1988.
6. P. PEGON, P. GUELIN, *On thermomechanical Zaremba schemes of hysteresis*, Res Mechanica, 21, 21–34, 1987.
7. D. FAVIER, P. GUELIN and P. PEGON, *Thermomechanics of hysteresis effects in shape memory alloys*, Int. Conf. on Martensitic Transformation, Sydney 1989.
8. A. TOURABI, B. WACK and D. FAVIER, *Experimental determination of the hysteresis properties in shape memory alloys*, Int. Conf. on Martensitic Trans., Sydney 1989.
9. C. DE CARBON, *Deformation des solides*, Comptes Rendus Académie des Sciences à Paris, vol.216, 241–244, 1942.
10. B. PERSOZ, *Modèles non linéaires*, La Rhéologie, III, 45–72, Masson, Paris 1969.
11. P. GUELIN, *Remarques sur l'hystérésis mécanique*, J.de Méca., 19, 2, 217–247, 1980.
12. E. DEGNY, *Etude du comporement d'un sable dense à l'aide d'une presse tridimensionnelle*, Thèse, Grenoble 1984.
13. B. WACK, F. LOUCHET and A. TOURABI, *Comporement d'hystérésis pure et passage micro-macro qualitatif*, Colloque de Plasticité 88, Grenoble 1988.
14. D. FAVIER, P. GUELIN, F. LOUCHET, P. PEGON, A. TOURABI and B. WACK, *Microstructural origin of hysteresis and application to continuum modelling of solid behaviour*, Continuum Models and Discrete System, Ed. Maugin, Longman, 110–119, 1990.

COMMISSION OF THE EUROPEAN COMMUNITIES
JOINT RESEARCH CENTRE, ISPRA, ITALY,
INSTITUTE OF MECHANICS, GRENOBLE, FRANCE,
GENIE PHYSIQUE ET MECANIQUE DES MATERIAUX, ST MARTIN D'HERES, FRANCE,
AND
POLISH ACADEMY OF SCIENCES,
INSTITUTE OF FUNDAMENTAL TECHNOLOGICAL RESEARCH.

Received September 12, 1990.